Journal Pre-proof

Formulations that suppress aggregation during long-term storage of a bispecific antibody are characterized by high refoldability and colloidal stability

Hristo L. Svilenov, Gerhard Winter

PII: S0022-3549(20)30137-4

DOI: https://doi.org/10.1016/j.xphs.2020.03.011

Reference: XPHS 1902

To appear in: *Journal of Pharmaceutical Sciences*

Received Date: 8 December 2019

Revised Date: 6 February 2020

Accepted Date: 12 March 2020

Please cite this article as: Svilenov HL, Winter G, Formulations that suppress aggregation during long-term storage of a bispecific antibody are characterized by high refoldability and colloidal stability, *Journal of Pharmaceutical Sciences* (2020), doi: https://doi.org/10.1016/j.xphs.2020.03.011.

Formulations that suppress aggregation during long-term storage of a bispecific antibody are characterized by high refoldability and colloidal stability

Hristo L. Svilenov*, Gerhard Winter

Department of Pharmacy, Pharmaceutical Technology and Biopharmaceutics, Ludwig-Maximilians University, Butenandtstrasse 5-13, Munich D-81377, Germany

*Corresponding author:

Hristo L. Svilenov

Email: hrisph@cup.uni-muenchen.de

ORCID: https://orcid.org/0000-0001-5863-9569

KEYWORDS: Protein formulation(s); Protein refolding; Protein aggregation; Light scattering (dynamic); Light scattering (static); Physical stability;

ABBREVIATIONS:

A_2 - second virial coefficient from static light scattering;

Bis-mAb – bispecific IgGκ-scFv antibody used in this work;

$C_{1/2}$ - melting denaturant concentration;

ICD - isothermal chemical denaturation;

k – aggregation rate constant;

k_D - interaction parameter from dynamic light scattering;

MWCO - molecular weight cut-off;

RMY - relative monomer yield;

scFv - single-chain variable domain;

SvP - subvisible particles;

ABSTRACT:

Understanding the formulation features that ensure sufficient stability during long-term storage is critical for developing next-generation therapeutic proteins. In this work, we investigate the physical stability of a bispecific antibody (Bis-mAb) in 12 different formulation conditions. Isothermal chemical denaturation with urea indicates a higher resistance to denaturant-induced unfolding when pH is increased from 5.0 to 6.5 but shows minor influence from the buffer type and ionic strength. Dynamic and static light scattering are used to derive the interaction parameter (k_D) and second virial coefficient (A_2), respectively. These two parameters indicate that Bis-mAb exhibits highest colloidal stability in formulations containing 10 mM histidine buffer without added sodium chloride. Further, we observe that the highest relative monomer yield (RMY) after isothermal refolding, i.e. the highest refoldability, from urea is measured for the low ionic strength histidine formulations. Finally, we show long-term stability data on all 12 Bis-mAb formulations after storage at 4 and 25 °C for 12 months. The least amount of soluble aggregates and subvisible particles were detected in the Bis-mAb formulations with the highest colloidal stability and refoldability from urea. We suggest that the optimization of these two features is crucial for obtaining physically stable formulations of Bis-mAb.

INTRODUCTION

Bispecific antibodies are becoming increasingly popular as therapeutic proteins because they can simultaneously address different antigens[1,2]. Such proteins are typically a result of protein engineering efforts and can be different from the canonical Y-shaped human IgG structure. One example of engineered bispecific antibodies is the IgGs with additional single-chain variable domains (scFvs)[3]. The complexity of an IgG-scFv is needed to obtain certain desired biological features[3]. However, such artificially-created protein structures can exhibit reduced physical stability and increased aggregation propensity during storage in comparison to naturally occurring IgGs[4,5].

The aggregation during storage of an IgG-scFv can be reduced by using suitable formulation conditions[3,5]. A set of formulations must be tested to find the optimal formulation conditions, e.g. pH and ionic strength, that stabilize a new protein. Such testing can be based either on lengthy and expensive stress and accelerated stability studies or on biophysical techniques that provide parameters describing protein physical stability[6,7].

The application and usefulness of short-term biophysical characterization to predict aggregation during storage were investigated for various proteins, e.g. cytokines[8–10], IgGs[11–21], dual-viable domain IgG[22] and others[13,23–25]. These case studies often show contradicting conclusions whether biophysical parameters describing protein conformational and colloidal stability can or cannot provide reasonable predictions for protein storage stability. These contradictions have been confusing for the community and led to the adoption of different philosophies about the most rational way to select protein formulations that will move on towards long-term stability studies.

Now it becomes more apparent that the optimization of specific biophysical parameters (e.g. melting temperature) is useful for protein development only until a mechanistic limit of a parameter is reached[26]. The mechanistic limits and weight of the different stability parameters will most probably differ even within the same class of proteins (e.g. IgGs), which would explain the discrepancies found in the literature. The considerations mentioned above open two significant questions that will be important for the future optimization of the protein formulation process: 1. Are there novel methods that can provide reasonable predictions for the aggregation of proteins during long-term storage when the mechanistic limits of some biophysical parameters are reached?; and 2. Which biophysical parameters provide truly orthogonal information, and what is the most rational set of biophysical parameters to predict formulations that suppress protein aggregation during storage qualitatively?

The present work focuses on several methods for biophysical characterization that are well-established (i.e. isothermal chemical denaturation and dynamic light scattering) or emerging (e.g. assessment of aggregation during refolding from a denaturant and static light scattering in multiwell plates) as tools to qualitatively predict the physical storage stability of proteins in different formulation conditions. We apply these methods to 12 formulations of a model protein, a bispecific IgG-scFv. The latter represents a class of therapeutically relevant molecules that are rarely used in published work, aiming to elucidate the relationships between biophysical parameters and long-term storage stability. We discuss whether the measured biophysical parameters provide orthogonal information for the physical stability of the formulations. Finally, we also show how the stability rankings based on different biophysical parameters correlate with long-term stability data obtained after storage for 12 months at 4 and 25 °C.

MATERIALS AND METHODS

Protein and materials

The bispecific antibody (Bis-mAb) used in this work is a human IgG1κ-scFv. The protein molecular mass is 204.4 kDa, its isoelectric point is around 9. Bis-mAb was supplied at concentration 50 mg/mL in a surfactant-free bulk buffer, which was exchanged by extensive dialysis against 10 mM histidine/histidine hydrochloride or 10 mM citric acid/sodium citrate buffer with pH 5.0, 5.75 or 6.5. Protein concentration was determined with spectrophotometry at 280 nm using a NanoDrop 2000 (Thermo Fisher Scientific) and the respective extinction coefficient. Sodium chloride was spiked in the dialyzed Bis-mAb samples from stock solutions prepared with the corresponding buffers. Values for the ionic strength of each formulation condition are provided in Table S1.

All chemicals were high purity grade and were purchased from Sigma Aldrich, Fisher Scientific or VWR International. Ultrapure water (arium® system, Sartorius Lab Instruments) was used for preparing all solutions.

Isothermal chemical denaturation

Isothermal chemical denaturation (ICD) was performed using a previously described semi-automated method[27]. Dialyzed Bis-mAb, the respective formulation buffer and 10 M urea solution in this buffer were combined with a Viaflo Assist system (Integra Biosciences) in 384 non-binding surface multiwell plates (Corning). After mixing, the samples were incubated for 24 hours at room temperature. Subsequently, the intrinsic protein fluorescence intensity at 330 and 350 nm was measured after

excitation at 280 nm with a FLUOstar® Omega microplate reader (BMG Labtech). To obtain the isothermal chemical denaturation curves, we plotted the intrinsic protein fluorescence intensity ratio FI350/FI330 against the urea concentration. Origin 2018 was used to apply a Boltzmann fit to the curves and derive the melting denaturant concentration ($C_{1/2}$) at 50 % threshold of the signal change.

Dynamic light scattering

All samples were prepared by centrifugation for 10 minutes at 10,000g. Afterwards, 50 µL Bis-mAb solution with different protein concentration in the respective formulation was filled in a Corning® high content imaging 384 microwell plate. The plate was centrifuged at 2200 rpm for 2 minutes using a Heraeus Megafuge 40 centrifuge equipped with an M-20 well plate rotor (Thermo Fisher Scientific). Next, each well was sealed with 10 µL silicon oil and the plate was centrifuged again as described above. The dynamic light scattering (DLS) measurements were performed at 25 °C with a DynaPro plate reader III (Wyatt Technology) and the Dynamics V7.8 software from the same company. The measurement of each sample consisted of 10 acquisitions of 5 s, with enabled auto-attenuation. Cumulant analysis was used to derive the mutual diffusion coefficient and polydispersity index from the autocorrelation functions. The interaction parameter k_D was determined from the concentration dependence of the mutual diffusion coefficient using the following equation:

$$D = D_0(1 + k_D c)$$

where D_0 is the diffusion coefficient at infinite dilution and c is the protein concentration. All DLS measurements were performed in triplicates.

Static light scattering

The samples were prepared in the same way as for DLS (see above), with the only difference that the wells were not sealed with silicon oil before measurements. The static light scattering (SLS) was measured with a DynaPro plate reader III (Wyatt Technology) operated with the Dynamics V7.8 software. Each well was measured at 25 °C with 10 acquisitions of 3 s. The laser power was adjusted to 20 % and the auto-attenuation to 0 %. The respective buffers without protein were measured to determine the solvent offsets. The Corning® high content imaging 384 microwell plates were calibrated using different concentrations of a dextran standard with known molecular mass and second virial coefficient A_2.

For isotropic scatterers like small proteins, the second virial coefficient can be derived from the following form of the Zimm equation[28,29]:

$$\frac{Kc}{R(\theta)} = \frac{1}{M} + 2A_2c$$

where $R(\theta)$ represents the excess Rayleigh ratio of the protein solution over the solvent, c is the protein concentration, M is the weight-averaged protein molecular mass, A_2 is the second virial coefficient, K is a constant ($K = 4\pi^2 n_0^2 (\mathrm{dn/dc})^2/(N_a \lambda_0^4)$), where n_0 is the solvent refractive index, dn/dc is the protein refractive index increment, N_a is the Avogadro's number, λ_0 is the laser wavelength in vacuum). The calculations to derive the second virial coefficient of Bis-mAb were done with the Dynamics V7.8 software using a dn/dc value of 0.185 mL/g.

Isothermal unfolding and refolding with urea (ReFOLD assay)

A previously presented ReFOLD assay was used to assess the effect of the formulation conditions on the isothermal aggregation of Bis-mAb after refolding from a denaturant[30]. Pierce™ microdialysis devices (membrane with 3.5 kDa MWCO) were used to dialyse 50 µL of formulated Bis-mAb with 5 mg/mL concentration against 1.5 mL of 10 M urea solution prepared in the respective formulation buffer. The urea solution was changed 4 and 8 hours after the start. The dialysis continued for 24 hours. Subsequently, the same dialysis procedure was repeated against the denaturant-free formulation buffer. Dialysis was performed in 96 deep multiwell plates with continuous agitation at 700 rpm using a Thermomixer Comfort (Eppendorf AG). After all dialysis steps, the samples were collected, each sample was weighed on a microbalance, and its weight was adjusted to 250 mg with the respective denaturant-free formulation buffer. The samples were centrifuged at 10,000g for 10 minutes. The supernatant was used for analysis with size-exclusion chromatography coupled to multi-angle light scattering (SEC-MALS). The SEC-MALS set-up consisted of a Dionex UltiMate 3000 UHPLC system with a UV-Vis absorbance detector (Thermo Fisher Scientific), a DAWN HELEOS multi-angle static light scattering detector (Wyatt Technology) and a TSKgel G3000SWxl, 7.8×300 mm, 5 µm column (Tosoh Bioscience). The running buffer had a pH of 7.0 and contained 100 mM potassium phosphate, 200 mM sodium chloride and 0.05 % w/v sodium azide. A flow of 0.5 mL/min and an injection volume of 50 µL were used. The concentration of the eluted samples was monitored at 280 nm. The molecular weight was calculated in the Astra v7.1 software (Wyatt Technology) from the UV and MALS signals using the protein extinction coefficient and the Zimm model. Chromeleon V7 (Thermo Fisher Scientific) was used to integrate the chromatograms and calculate the monomer area from the UV signal. The relative monomer yield (RMY) was calculated by dividing the monomer area of a sample after refolding from urea by the monomer area of the sample before the refolding.

Long-term stability study

Formulated Bis-mAb samples with concentration 5 mg/mL were sterile filtered using a 0.22 µm cellulose acetate filter and aseptically filled into sterile DIN2R glass type I vials (MGlass AG). The vials were crimped with FluroTec® coated rubber chlorobutyl stoppers (West Pharmaceutical Services) and stored at 4 and 25 °C. Three different vials were used for the analysis of each time point, formulation condition and storage temperature.

To assess the formation of small soluble aggregates during storage, we used size exclusion chromatography (SEC) on a Dionex Summit 2 HPLC system (Thermo Fisher Scientific). The sample elution was monitored at 280 nm with a UVD170U UV/Vis detector. The column and running buffer were the same as for the SEC-MALS method described earlier. Chromeleon V6.8 (Thermo Fisher Scientific) was used to integrate the chromatograms and to calculate the relative area of the aggregates related to the area of all protein peaks. The monomer recovery was calculated as the area of the monomer peak after storage was divided by the area of the monomer peak measured at the start of the stability study.

Flow imaging microscopy was employed for assessing the number and size of subvisible particles (SvP) formed during storage. A FlowCAM® 8100 with the VisualSpreadsheet® 4.7.6 software (Fluid Imaging Technologies) was used for data collection and analysis. The device was equipped with a 10x magnification cell (81 µm x 700 µm). The sample volume was 150 µL, the flow rate was 0.15 mL/min, the auto image frame rate was 29 frames/second, and the sampling time was 74 seconds. The particle identification settings were 3 µm distance to the nearest neighbor, particle segmentation thresholds of 13 and 10 for the dark and light pixels respectively. The reported particle size is the equivalent spherical diameter (ESD).

RESULTS AND DISCUSSION

The resistance to urea-induced unfolding of Bis-mAb depends mostly on pH

Isothermal chemical denaturation was selected to study the conformational stability of Bis-mAb because the protein was formulated in buffers that exhibit different pH shifts during heating, thus complicating the rankings based on melting temperatures[27]. As the formulation pH is increased from 5.0 to 6.5, higher urea concentration is needed to cause structural perturbations of Bis-mAb (Figure 1). The unfolding of Bis-mAb in urea is not completely reversible, and the degree of reversibility depends strongly on the formulation conditions (see below). Therefore, the thermodynamic analysis and extraction of Gibbs free energy of unfolding from the ICD curves would be inaccurate[31]. A further complication for the analysis is that Bis-mAb does not exhibit clearly defined transitions that can be well described by a two-state or a three-state unfolding model (data not shown). For these reasons, we fitted the obtained ICD curves using a Boltzmann function and derived denaturant melting concentrations ($C_{1/2}$) that indicate the resistance to urea-induced unfolding in different formulation conditions (Figure 1). Similar approaches that employ ICD to determine relative $C_{1/2}$ values are shown to be predictive for the storage stability of some proteins[32]. The differences in the $C_{1/2}$ between conditions, i.e. different buffers and ionic strengths, with the same pH are only minimal, within 0.1-0.2 M urea (Table 1). In comparison, pH has a much larger effect on the $C_{1/2}$ of Bis-mAb – an increase in pH from 5.0 to 6.5 shifts the $C_{1/2}$ by approximately 0.6-0.7 M in both histidine- and citrate-based formulations, regardless of the ionic strength.

The colloidal stability of Bis-mAb depends on the buffer type and addition of sodium chloride

The mutual diffusion coefficient of Bis-mAb was determined at different protein concentrations and in different formulation conditions (Figure 2). In formulations with 10 mM histidine buffer without added sodium chloride, the D_0 increases with increasing protein concentration regardless of the pH (Figure 2a). In all other formulation conditions, the mutual diffusion coefficient decreases with increasing Bis-mAb concentration. Correspondingly, the interaction parameter k_D is highest in the low ionic strength histidine formulations and negative in all other conditions (Table 1). The high k_D can be attributed to strong electrostatic repulsion between the monomers. The formulations containing 10 mM citrate without added sodium chloride also have relatively low ionic strength but exhibit much lower k_D compared to histidine counterparts. These effects can be explained by the binding of the citrate ion to the protein that inverts protein surface charge and diminishes the electrostatic repulsion[33,34]. The

addition of 70 mM NaCl levels out the differences in k_D of Bis-mAb in the two different buffers (see Figure 2) due to screening of the electrostatic interactions[35].

The static light scatting results closely resemble the dynamic light scattering data (Figure 3). The second virial coefficient A_2 of Bis-mAb is highest in the 10 mM histidine formulations without added salt (Figure 3a and Table 1). In all other conditions, A_2 is significantly lower, but contrary to k_D does not reach negative values upon screening of the electrostatic repulsion (Table 1). Both the good correlation and the offset between A_2 and k_D are well known for monoclonal antibodies and the reasons for them have been elucidated[35,36]. This agreement between k_D and A_2 is also valid for the formulations of the bispecific antibody used in this work.

The formulation conditions affect Bis-mAb aggregation during refolding from urea

The freshly prepared Bis-mAb formulations contain more than 95 % monomer and a fraction of dimer in all 12 conditions (see below). After isothermal refolding from urea, a significant amount of the protein monomer is lost and aggregates of various sizes from dimer to multimers can be detected with SEC-MALS (Figure 4a). The highest relative monomer yield, i.e. highest refoldability, is detected in 10 mM histidine formulations without additional NaCl (Figure 4b). This indicates that the least amount of Bis-mAb monomer aggregates through non-native interactions in these three conditions. Formulations containing 10 mM citrate buffer or 70 mM sodium chloride show dramatically lower relative monomer yield (Figure 4b), indicating the high aggregation propensity of the (partially) unfolded Bis-mAb in these conditions. Noteworthy, Bis-mAb has lower much lower RMYs compared to three IgGs that were studied at similar protein concentration in the same formulation conditions, indicating that this bispecific antibody is very prone to aggregation during refolding[30,37]. Whether bispecifics have lower refoldability compared to analogical antibodies with canonical IgG structure is yet to be investigated.

Bis-mAb forms soluble aggregates and subvisible particles during long-term storage

The long-term stability studies were performed for 12 months at 4 and 25 °C. At the designated sampling points, the relative area of aggregates was assessed with size exclusion chromatography (Figure 5). Bis-mAb formulations already contain slightly different amount of aggregates at the beginning of the stability study, which indicates that the formulation conditions have an impact on the self-association of the protein that is quickly evident within the timeframe between sample preparation and SEC analysis (less than 5 days at 4 °C). The smallest change in the relative area of aggregates was observed for the 10 mM histidine formulations, regardless of the pH, during

storage at 4 and 25 °C (Figure 5a and 5b). In all other cases, the relative aggregate area increased more during long-term storage. Interestingly, Bis-mAb formed an almost similar amount of aggregates during storage at 4 and 25 °C, which might be due to protein aggregation that follows non-Arrhenius behaviour[38]. In the present work, we do not have enough experimental data to calculate aggregation rates at different temperatures accurately to confirm this theory. However, non-Arrhenius aggregation is typical for folded monomeric proteins (like Bis-mAb), and a concave up ln*k* versus 1/T dependence can explain similar aggregation rates at 4 and 25 °C. More information about the reasons of non-Arrhenius protein aggregation behaviour can be found in the literature[38–41].

Considerable numbers of subvisible particles were formed during storage in most Bis-mAb formulations (Figure 6). The lowest numbers of SvP were detected in the 10 mM histidine formulations with low ionic strength (Figure 6a). In general, there is a trend that the formulations that contain 70 mM NaCl formed more subvisible particles (Figure 6c, 6d, 6g and 6h) compared to counterparts with lower ionic strength (Figure 6a, 6b, 6e and 6f). These observations are in accordance with the effect of ionic strength on the aggregate size formed by other proteins when the electrostatic repulsion between monomers is screened[42].

In general, Bis-mAb forms more soluble aggregates and subvisible particles during long-term storage compared to two IgGs that we studied at similar formulation and storage conditions[30]. This observation concurs well with the lower RMYs of the bispecific antibody compared to the IgGs from previous work. Although the currently published data is limited to make conclusions in this direction, it seems that less physically stable proteins could have lower refoldability. Therefore, future studies should focus on the importance of refoldability for the selection of developable protein drug candidates.

Colloidal stability and refoldability correlate with Bis-mAb aggregation during storage

Looking for connections between biophysical parameters (measured in short timeframes) and the information obtained during long-term stability studies at 4 and 25 °C, we compared some of the values presented above. We depicted both linear correlations with their 95 % confidence ellipses and Spearman`s rank correlation coefficients (*R*) between the mean values of biophysical parameters and long-term stability data obtained for the formulations (Figure 7).

The strongest correlation between biophysical parameters that we observe is between k_D and A_2 (Figure 7), which is already reported for other proteins[35,36]. Interestingly, the *R* between k_D (or A_2) and the relative monomer yield from the ReFOLD assay is below the threshold for significance.

Although all these three parameters indicate high physical stability of Bis-mAb in the 10 mM histidine formulations without NaCl, the exact stability ranking based on k_D (or A_2) and the RMY is different. There is also a strong correlation between D_0 and M_m (Figure 7) which appears logical as both parameters will be affected by the presence of a small aggregate population that was detected in all samples with size exclusion chromatography.

When we compare the biophysical parameters that can be assessed in short timeframes to the long-term stability studies, we observe several significant rank correlations. First, the interaction parameter k_D and the second virial coefficient A_2 correlate with the relative area of aggregates formed after 12 months of storage at 4 and 25 °C (Figure 7). Second, the RMY from the ReFOLD assay shows very strong rank correlation with the relative area of aggregates and the monomer loss after 12 months at 25 °C (Figure 7). There is also a moderate correlation between RMY and the monomer loss at 4 °C (the rank correlation between RMY and the relative area of aggregates at 4 °C is just below the threshold to be considered significant). And third, the melting denaturant concentration $C_{1/2}$ correlates significantly only with the monomer loss after storage at 25 °C (Figure 7).

We also observe several significant ranking correlations between long-term stability data. For example, the rankings for aggregates, monomer loss and subvisible particles obtained after storage at 25 °C correlate well with the rankings based on these parameters measured after storage at 4 °C. These findings support a recent publication that discusses the practicality of accelerated stability studies at different temperatures to predict protein aggregation during long-term storage under refrigerated conditions[43].

An interesting observation is that the diffusion coefficient at infinite dilution D_0 was the only biophysical parameter that shows a significant correlation with the number of subvisible particles (Figure 7). A possible explanation here might be that some of the soluble aggregates in samples prone to form subvisible particles were quickly depleted by forming larger aggregates. The latter were then removed during the centrifugation step before the DLS analysis. This will result in a larger fraction of soluble aggregates, respectively lower D_0, in formulation conditions where the formation of SvP is suppressed.

Although it is interesting to look into the linear and rank correlations between the parameters, we should underline that the formulations of Bis-mAb that exhibited the lowest aggregation and SvP formation during storage, were clearly the formulations that have significantly higher colloidal stability (based on k_D and A_2 values) and refoldability (based on RMY after refolding from urea) (see Table 1).

In contrast, formulations with higher $C_{1/2}$ values did not exhibit better storage stability in most cases. This indicates that the $C_{1/2}$ values of all 12 Bis-mAb formulations are most probably already above the mechanistic limit of this parameter. Thus, making $C_{1/2}$ not predictive for the aggregation during long-term storage of these formulations.

Refoldability and colloidal stability studies provide orthogonal information

We previously showed that assessing the aggregation during dilution- or dialysis-refolding from denaturants can be a valuable tool to select monoclonal antibody formulations with higher physical stability and suppressed aggregation during storage[30,37,44]. In an effort to standardize such experiments, we presented a ReFOLD assay that is based on microdialysis in deep multiwell plates[30]. We demonstrated that assessing the effect of the formulation on the protein monomer yield (i.e. the fraction of monomer that is not aggregated after unfolding and refolding with urea) from the ReFOLD assay is a valuable approach to qualitatively predict the physical storage stability of three different antibodies in various formulation conditions[30,37]. In the study presented here, we applied this concept to a different molecule – the bispecific antibody Bis-mAb which is a human IgG1κ-scFv protein. We found that the formulation conditions that lead to the highest relative monomer yield after refolding from urea are the formulations that impede aggregation and subvisible particle formation of Bis-mAb during long-term storage for 12 months at 4 and 25 °C.

The aggregation after refolding from denaturants of some proteins is related to parameters describing the colloidal protein stability in the presence in denaturants[45,46]. In our work, we also focused on two widely used parameters that describe the protein-protein interactions in solution[45,46]. We found that Bis-mAb formulations that have significantly higher second virial coefficient A_2 and interaction parameter k_D in the absence of denaturants are the formulations that have the highest relative monomer yield after refolding from urea. However, there was no significant rank correlation between k_D (or A_2) and the RMY, indicating that although these biophysical parameters are connected, they carry different and complementary information. We also recently reported a similar interplay between k_D, A_2 and RMY for an IgG antibody[37].

The colloidal stability of the native state is undoubtedly crucial for obtaining formulations with suppressed aggregation during storage. However, the effect of the formulation on the aggregation propensity of the partially unfolded protein at ambient temperatures also seems to play an important role for several IgGs and in this case for a bispecific antibody. This aggregation propensity can be quickly assessed by using an unfolding/refolding experimental setup like the ReFOLD assay, or by

measuring the second virial coefficient or the aggregation of a protein in the presence of denaturants[45,47,48]. Such experiments with denaturants offer several advantages over traditional thermal denaturation methods, as they do not require sample heating and result in more moderate aggregation of the partially unfolded protein that allows comparisons between the effect of the formulation on the non-native protein aggregation[27,30]. Currently, we are limited by the fact that we cannot observe the unfolding/refolding and aggregate formation in the dialysis device as the denaturant concentration is changed. To this end, we are focusing on experimental setups that allow automated microdialysis with in situ detection of protein conformational changes and aggregation. We believe that such setups will provide a better understanding of the concept behind the ReFOLD assay.

CONCLUSIONS

In this work, we applied several methods to study the physical stability of a bispecific antibody in 12 formulation conditions. In addition, we performed long-term stability studies for 12 months at 4 and 25 °C to investigate whether some of the assessed biophysical parameters can provide qualitative predictions for the aggregation of Bis-mAb in different formulations. We observe a strong correlation between A_2 and k_D, but no significant rank correlation between either of these two parameters and the relative monomer yield after refolding from urea. These findings suggest that assessing the colloidal stability of the native protein and studying the aggregation during refolding from denaturants are two orthogonal approaches. Both of the latter show reasonable predictions for the ranking of Bis-mAb formulations in order of their effect on protein aggregation during long-term storage. These findings add to our earlier reports with formulations of three IgGs[30,37], further supporting the hypothesis that the high reversibility of isothermal protein unfolding (induced by denaturants like urea) is a key feature of physically stable formulations of therapeutic proteins.

ACKNOWLEDGEMENTS

This study was funded by a project part of the EU Horizon 2020 Research and Innovation program under the Marie Skłodowska-Curie grant agreement No 675074.

REFERENCES

1. Kontermann RE, Brinkmann U. Bispecific antibodies; different formats. *Drug Discov Today*. 2015;20(7):838-847. doi:10.1016/j.drudis.2015.02.008

2. Baeuerle PA, Reinhardt C. Bispecific T-cell engaging antibodies for cancer therapy. *Cancer Res*. 2009;69(12):4941-4944. doi:10.1158/0008-5472.CAN-09-0547

3. US20180022807A1 - Bispecific binding proteins and uses thereof - Google Patents. https://patents.google.com/patent/US20180022807A1/en. Accessed November 9, 2019.

4. Wang Q, Chen Y, Park J, et al. Design and Production of Bispecific Antibodies. *Antibodies*. 2019;8(3):43. doi:10.3390/antib8030043

5. Manikwar P, Mulagapati SHR, Kasturirangan S, Moez K, Rainey GJ, Lobo B. Characterization of a Novel Bispecific Antibody With Improved Conformational and Chemical Stability. *J Pharm Sci*. July 2019. doi:10.1016/j.xphs.2019.06.025

6. Manning MC, Liu J, Li T, Holcomb RE. *Rational Design of Liquid Formulations of Proteins*. Vol 112. Academic Press; 2018:1-59. doi:10.1016/bs.apcsb.2018.01.005

7. Wang W, Ohtake S. Science and art of protein formulation development. *Int J Pharm*. 2019;568:118505. doi:10.1016/j.ijpharm.2019.118505

8. Youssef AMK, Winter G. A critical evaluation of microcalorimetry as a predictive tool for long term stability of liquid protein formulations: Granulocyte Colony Stimulating Factor (GCSF). *Eur J Pharm Biopharm*. 2013;84(1):145-155. doi:10.1016/j.ejpb.2012.12.017

9. Maddux NR, Iyer V, Cheng W, et al. High throughput prediction of the long-term stability of pharmaceutical macromolecules from short-term multi-instrument spectroscopic data. *J Pharm Sci*. 2014;103(3):828-839. doi:10.1002/jps.23849

10. Svilenov H, Winter G. Rapid sample-saving biophysical characterisation and long-term storage stability of liquid interferon alpha2a formulations: Is there a correlation? *Int J Pharm*. 2019;562:42-50. doi:10.1016/j.ijpharm.2019.03.025

11. Goldberg DS, Bishop SM, Shah AU, Sathish HA. Formulation Development of Therapeutic Monoclonal Antibodies Using High-Throughput Fluorescence and Static Light Scattering

Techniques: Role of Conformational and Colloidal Stability. *J Pharm Sci*. 2011;100(4):1306-1315. doi:10.1002/jps.22371

12. Goldberg DS, Lewus RA, Esfandiary R, et al. Utility of High Throughput Screening Techniques to Predict Stability of Monoclonal Antibody Formulations During Early Stage Development. *J Pharm Sci*. 2017;106(8):1971-1977. doi:10.1016/j.xphs.2017.04.039

13. Bajaj H, Sharma VK, Badkar A, Zeng D, Nema S, Kalonia DS. Protein structural conformation and not second virial coefficient relates to long-term irreversible aggregation of a monoclonal antibody and ovalbumin in solution. *Pharm Res*. 2006;23(6):1382-1394. doi:10.1007/s11095-006-0018-y

14. Brader ML, Estey T, Bai S, et al. Examination of thermal unfolding and aggregation profiles of a series of developable therapeutic monoclonal antibodies. *Mol Pharm*. 2015;12(4):1005-1017. doi:10.1021/mp400666b

15. He F, Hogan S, Latypov RF, Narhi LO, Razinkov VI. High throughput thermostability screening of monoclonal antibody formulations. *J Pharm Sci*. 2010;99(4):1707-1720. doi:10.1002/jps.21955

16. Thiagarajan G, Semple A, James JK, Cheung JK, Shameem M. A comparison of biophysical characterization techniques in predicting monoclonal antibody stability. *MAbs*. 2016;8(6):1088-1097. doi:10.1080/19420862.2016.1189048

17. Cheng W, Joshi SB, He F, et al. Comparison of high-throughput biophysical methods to identify stabilizing excipients for a model IgG2 monoclonal antibody: conformational stability and kinetic aggregation measurements. *J Pharm Sci*. 2012;101(5):1701-1720. doi:10.1002/jps.23076

18. Barnett G V., Razinkov VI, Kerwin BA, Hillsley A, Roberts CJ. Acetate- and Citrate-Specific Ion Effects on Unfolding and Temperature-Dependent Aggregation Rates of Anti-Streptavidin IgG1. *J Pharm Sci*. 2016;105(3):1066-1073. doi:10.1016/j.xphs.2015.12.017

19. Fesinmeyer RM, Hogan S, Saluja A, et al. Effect of ions on agitation- and temperature-induced aggregation reactions of antibodies. *Pharm Res*. 2009;26(4):903-913. doi:10.1007/s11095-008-9792-z

20. Saito S, Hasegawa J, Kobayashi N, Tomitsuka T, Uchiyama S, Fukui K. Effects of ionic

strength and sugars on the aggregation propensity of monoclonal antibodies: Influence of colloidal and conformational stabilities. *Pharm Res*. 2013;30(5):1263-1280. doi:10.1007/s11095-012-0965-4

21. Alekseychyk L, Su C, Becker GW, Treuheit MJ, Razinkov VI. High-Throughput Screening and Stability Optimization of Anti-Streptavidin IgG1 and IgG2 Formulations. *J Biomol Screen*. 2014;19(9):1290-1301. doi:10.1177/1087057114542431

22. Kumar V, Dixit N, Zhou L, Fraunhofer W. Impact of short range hydrophobic interactions and long range electrostatic forces on the aggregation kinetics of a monoclonal antibody and a dual-variable domain immunoglobulin at low and high concentrations. *Int J Pharm*. 2011;421(1):82-93. doi:10.1016/j.ijpharm.2011.09.017

23. Shi S, Liu J, Joshi SB, et al. Biophysical characterization and stabilization of the recombinant albumin fusion protein sEphB4-HSA. *J Pharm Sci*. 2012;101(6):1969-1984. doi:10.1002/jps.23096

24. Remmele RL, Nightlinger NS, Srinivasan S, Gombotz WR. Interleukin-1 receptor (IL-1R) liquid formulation development using differential scanning calorimetry. *Pharm Res*. 1998;15(2):200-208. doi:10.1023/A:1011902215383

25. Espargaró A, Castillo V, de Groot NS, Ventura S. The in Vivo and in Vitro Aggregation Properties of Globular Proteins Correlate With Their Conformational Stability: The SH3 Case. *J Mol Biol*. 2008;378(5):1116-1131. doi:10.1016/j.jmb.2008.03.020

26. Robinson MJ, Matejtschuk P, Bristow AF, Dalby PA. Tm-Values and Unfolded Fraction Can Predict Aggregation Rates for Granulocyte Colony Stimulating Factor Variant Formulations but Not under Predominantly Native Conditions. *Mol Pharm*. 2018;15(1):256-267. doi:10.1021/acs.molpharmaceut.7b00876

27. Svilenov H, Markoja U, Winter G. Isothermal chemical denaturation as a complementary tool to overcome limitations of thermal differential scanning fluorimetry in predicting physical stability of protein formulations. *Eur J Pharm Biopharm*. 2018;125:106-113. doi:10.1016/j.ejpb.2018.01.004

28. Zimm BH. The scattering of light and the radial distribution function of high polymer solutions. *J*

Chem Phys. 1948;16(12):1093-1099. doi:10.1063/1.1746738

29. Wyatt PJ. Light scattering and the absolute characterization of macromolecules. *Anal Chim Acta*. 1993;272(1):1-40. doi:10.1016/0003-2670(93)80373-S

30. Svilenov H, Winter G. The ReFOLD assay for protein formulation studies and prediction of protein aggregation during long-term storage. *Eur J Pharm Biopharm*. 2019;137:131-139. doi:https://doi.org/10.1016/j.ejpb.2019.02.018

31. Wafer L, Kloczewiak M, Polleck SM, Luo Y. Isothermal chemical denaturation of large proteins: Path-dependence and irreversibility. *Anal Biochem*. 2017;539:60-69. doi:10.1016/j.ab.2017.10.001

32. Rizzo JM, Shi S, Li Y, et al. Application of a high-throughput relative chemical stability assay to screen therapeutic protein formulations by assessment of conformational stability and correlation to aggregation propensity. *J Pharm Sci*. 2015;104(5):1632-1640. doi:10.1002/jps.24408

33. Roberts D, Keeling R, Tracka M, et al. Specific Ion and Buffer Effects on Protein–Protein Interactions of a Monoclonal Antibody. *Mol Pharm*. 2015;12(1):179-193. doi:10.1021/mp500533c

34. Kalayan J, Henchman RH, Warwicker J. A Model for Counterion Binding and Charge Reversal on Protein Surfaces. *Mol Pharm*. December 2019 Accepted manuscript doi:10.1021/acs.molpharmaceut.9b01047

35. Roberts D, Keeling R, Tracka M, et al. The role of electrostatics in protein-protein interactions of a monoclonal antibody. *Mol Pharm*. 2014;11(7):2475-2489. doi:10.1021/mp5002334

36. Menzen T, Friess W. Temperature-ramped studies on the aggregation, unfolding, and interaction of a therapeutic monoclonal antibody. *J Pharm Sci*. 2014;103(2):445-455. doi:10.1002/jps.23827

37. Svilenov HL, Kulakova A, Zalar M, Golovanov AP, Harris P, Winter G. Orthogonal techniques to study the effect of pH, sucrose and arginine salts on monoclonal antibody physical stability and aggregation during long-term storage. *J Pharm Sci*. November 2019. doi:10.1016/j.xphs.2019.10.065

38. Wang W, Roberts CJ. Non-Arrhenius Protein Aggregation. *AAPS J*. 2013;15(3):840-851. doi:10.1208/s12248-013-9485-3

39. Wu H, Truncali K, Ritchie J, et al. Weak protein interactions and pH-and temperature-dependent aggregation of human Fc1. MAbs. 2015;7(6):1072-1083 doi:10.1080/19420862.2015.1079678

40. Kayser V, Chennamsetty N, Voynov V, Helk B, Forrer K, Trout BL. Evaluation of a non-arrhenius model for therapeutic monoclonal antibody aggregation. *J Pharm Sci*. 2011;100(7):2526-2542. doi:10.1002/jps.22493

41. Wang W, Nema S, Teagarden D. Protein aggregation-Pathways and influencing factors. *Int J Pharm*. 2010;390(2):89-99. doi:10.1016/j.ijpharm.2010.02.025

42. Roberts CJ. Therapeutic protein aggregation: Mechanisms, design, and control. *Trends Biotechnol*. 2014;32(7):372-380. doi:10.1016/j.tibtech.2014.05.005

43. Wälchli R, Vermeire P-J, Massant J, Arosio P. Accelerated Aggregation Studies of Monoclonal Antibodies: Considerations for Storage Stability. *J Pharm Sci*. 2020;109(1):595-602. doi:10.1016/j.xphs.2019.10.048

44. Svilenov H, Gentiluomo L, Friess W, Roessner D, Winter G. A New Approach to Study the Physical Stability of Monoclonal Antibody Formulations—Dilution From a Denaturant. *J Pharm Sci*. 2018;107(12):3007-3013. doi.org/10.1016/j.xphs.2018.08.004

45. Ho JGS, Middelberg APJ, Ramage P, Kocher HP. The likelihood of aggregation during protein renaturation can be assessed using the second virial coefficient. *Protein Sci*. 2003;12(4):708-716. doi:10.1110/ps.0233703.potential

46. Ho JGS, Middelberg APJ. Estimating the potential refolding yield of recombinant proteins expressed as inclusion bodies. *Biotechnol Bioeng*. 2004;87(5):584-592. doi:10.1002/bit.20148

47. Liu W, Cellmer T, Keerl D, et al. Interactions of lysozyme in guanidinium chloride solutions from static and dynamic light-scattering measurements. *Biotechnol Bioeng*. 2005;90(4):482-490. doi:10.1002/bit.20442

48. Austerberry JI, Thistlethwaite A, Fisher K, et al. Arginine to Lysine Mutations Increase the Aggregation Stability of a Single-Chain Variable Fragment through Unfolded-State Interactions.

Biochemistry. 2019;58(32):3413-3421. doi:10.1021/acs.biochem.9b00367

Figure legends

Figure 1*.Isothermal chemical denaturation curves of Bis-mAb at pH 5.0 (green squares), pH 5.75 (yellow circles) and pH 6.5 (red triangles) in (a) 10 mM histidine buffer without NaCl, (b) 10 mM histidine buffer with 70 mM NaCl, (c) 10 mM citrate buffer without NaCl and (d) 10 mM citrate buffer with 70 mM NaCl. Bis-mAb concentration is 0.5 mg/mL. The values are mean of triplicates, and the error is the standard deviation. The lines are a Boltzmann fit. The inset shows the residuals from the fit.*

Figure 2. *Effect of the formulation condition on the mutual diffusion coefficient of Bis-mAb at different protein concentrations - pH 5.0 (green squares), pH 5.75 (yellow circles) and pH 6.5 (red triangles) in (a) 10 mM histidine buffer without NaCl, (b) 10 mM histidine buffer with 70 mM NaCl, (c) 10 mM citrate buffer without NaCl and (d) 10 mM citrate buffer with 70 mM NaCl. The values are mean of triplicates, and the error is the standard deviation. The lines are linear fit to the data.*

Figure 3. *Effect of the formulation condition on the (Kc/(R(θ)) of Bis-mAb at different protein concentrations - pH 5.0 (green squares), pH 5.75 (yellow circles) and pH 6.5 (red triangles) in (a) 10 mM histidine buffer without NaCl, (b) 10 mM histidine buffer with 70 mM NaCl, (c) 10 mM citrate buffer without NaCl and (d) 10 mM citrate buffer with 70 mM NaCl. The values are mean of triplicates, and the error is the standard deviation. The lines are linear fit to the data.*

Figure 4. a *- SEC-MALS chromatogram of Bis-mAb before unfolding with urea (green triangles) and after isothermal refolding from urea (red squares);* ***b*** *– Effect of the formulation conditions on the relative monomer yield of Bis-mAb after isothermal refolding from urea;*

Figure 5*. Effect of the formulation conditions on the relative area of aggregates of Bis-mAb detected with size exclusion chromatography during storage at 4 °C (left column) and 25 °C (right column). Formulations with pH 5.0 (green squares), pH 5.75 (yellow circles) and pH 6.5 (red triangles) in (a, b) 10 mM histidine buffer without NaCl, (c, d) 10 mM histidine buffer with 70 mM NaCl, (e, f) 10 mM citrate buffer without NaCl and (g, h) 10 mM citrate buffer with 70 mM NaCl. The values are mean of triplicates, and the error is the standard deviation. The lines are guides for the eyes.*

Figure 6. *Effect of the formulation conditions on the cumulative number of subvisible particles ≥ 2 µm per mL of Bis-mAb detected with flow imaging microscopy during storage at 4 °C (left column) and 25 °C (right column). Formulations with pH 5.0 (green squares), pH 5.75 (yellow circles) and pH 6.5 (red triangles) in (a, b) 10 mM histidine buffer without NaCl, (c, d) 10 mM histidine buffer with 70 mM NaCl, (e, f) 10 mM citrate buffer without NaCl and (g, h) 10 mM citrate buffer with 70 mM NaCl. The values are mean of triplicates, and the error is the standard deviation. The lines are guides for the eyes.*

Figure 7. *Correlation between biophysical parameters of Bis-mAb (grouped in the blue square) and long-term stability data (grouped in the red square). The "% aggr. 25 °C" and the "% aggr. 4 °C" represent the relative area of aggregates from size exclusion chromatography detected after 12-month storage. The "% mon. 25 °C" and "% mon. 4 °C" represent the monomer recovery after 12-month storage. The "SvP 25 °C" and "SvP 4 °C" are the cumulative number of particles after 12 months of storage at the respective temperatures. The correlations are tested between the mean values of triplicates. The red lines are linear fits to the data, the red ellipses are the confidence ellipses at 95 % level. The empty squares for the Spearman`s rank correlation coefficient are cases where the rank correlation was not significant (p>0.05).*

Table 1. Biophysical parameters of Bis-mAb in different formulation conditions - melting denaturant concentration $C_{1/2}$ from isothermal chemical denaturation; second virial coefficient A_2 and molecular mass M_m from static light scattering; interaction parameter k_D and diffusion coefficient at infinite dilution D_0 from dynamic light scattering; relative monomer yield RMY from the ReFOLD assay; The values are mean of triplicates, and the error is the standard deviation.

Buffer	**pH**	**NaCl (mM)**	$C_{1/2}$ *(M)*	A_2 **(x10^{-4} mol.ml/g^2)**	M_m **(kDa)**	k_D **(x10^{-2} mL/mg)**	D_0 **(x10^{-7} cm^2/s)**	**RMY**
histidine	5.0	0	5.43 (±0.03)	2.81 (±0.08)	230 (±3.05)	3.407 (±0.26)	3.61 (±0.03)	0.295 (±0.008)
histidine	5.75	0	5.85 (± 0.02)	2.51 (±0.15)	230 (±5.71)	3.21 (±0.08)	3.63 (±0.01)	0.271 (±0.009)
histidine	6.5	0	6.16 (±0.01)	3.65 (±0.24)	232 (±7.85)	7.03 (±0.10)	3.55 (±0.01)	0.237 (±0.011)
histidine	5.0	70	5.32 (±0.07)	1.18 (±0.10)	231 (±4.71)	-0.347 (±0.17)	3.71 (±0.03)	0.029 (±0.003)
histidine	5.75	70	5.67 (±0.02)	0.67 (±0.05)	216 (±2.24)	-1.015 (±0.16)	3.77 (±0.03)	0.055 (±0.003)
histidine	6.5	70	5.96 (±0.03)	0.60 (±0.12)	226 (±5.70)	-1.393 (±0.20)	3.74 (±0.03)	0.058 (±0.002)
citrate	5.0	0	5.39 (±0.01)	1.06 (±0.14)	222 (±2.78)	-0.775 (±0.06)	3.83 (±0.02)	0.008 (±0.002)
citrate	5.75	0	5.81 (±0.02)	0.72 (±0.03)	213 (±1.74)	-0.908 (±0.14)	3.84 (±0.02)	0.020 (±0.004)
citrate	6.5	0	6.07 (±0.01)	0.56 (±0.01)	211 (±0.39)	-1.167 (±0.04)	3.87 (±0.01)	0.029 (±0.005)
citrate	5.0	70	5.29 (±0.04)	0.98 (±0.07)	229 (±2.90)	-0.748 (±0.03)	3.69 (±0.01)	0.005 (±0.001)
citrate	5.75	70	5.70 (±0.03)	0.76 (±0.05)	218 (±2.32)	-1.023 (±0.11)	3.76 (±0.04)	0.024 (±0.002)
citrate	6.5	70	6.06 (±0.03)	0.64 (±0.03)	215 (±1.77)	-1.267 (±0.22)	3.76 (±0.04)	0.040 (±0.002)

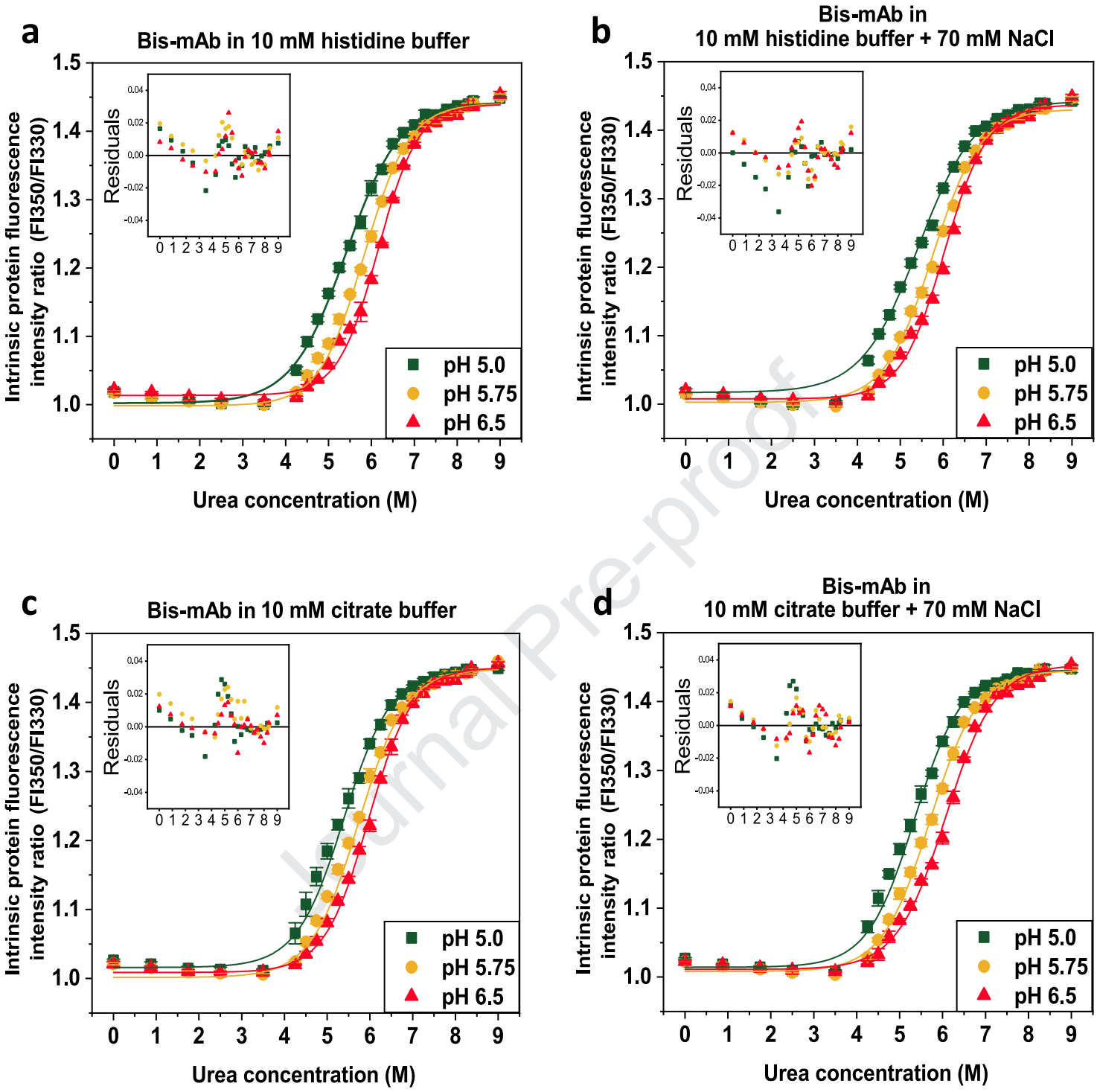

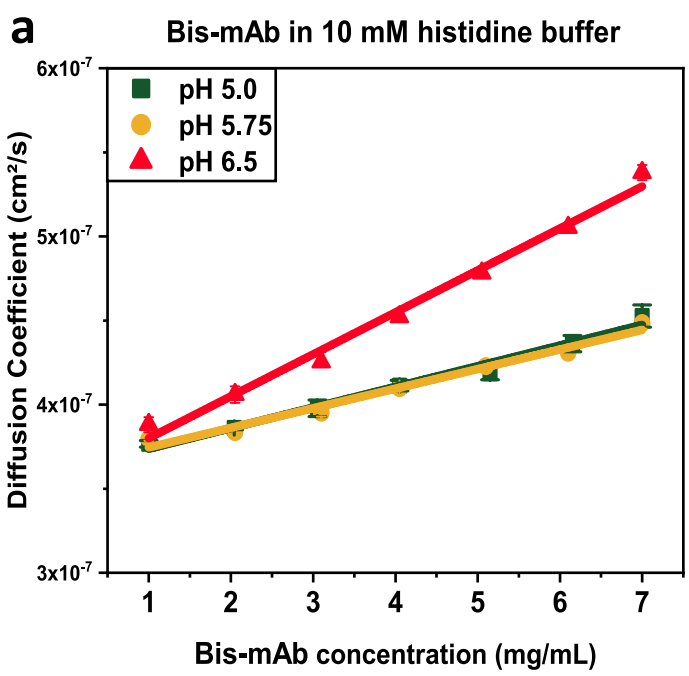

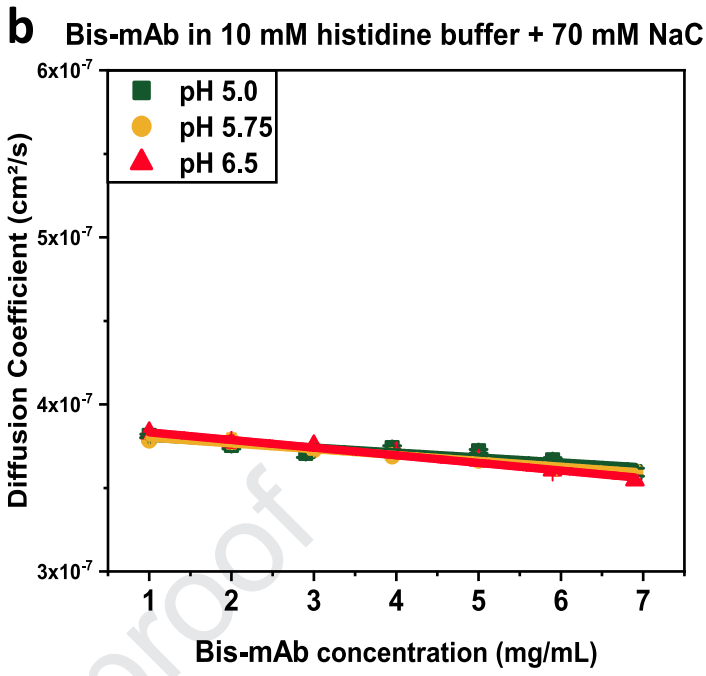

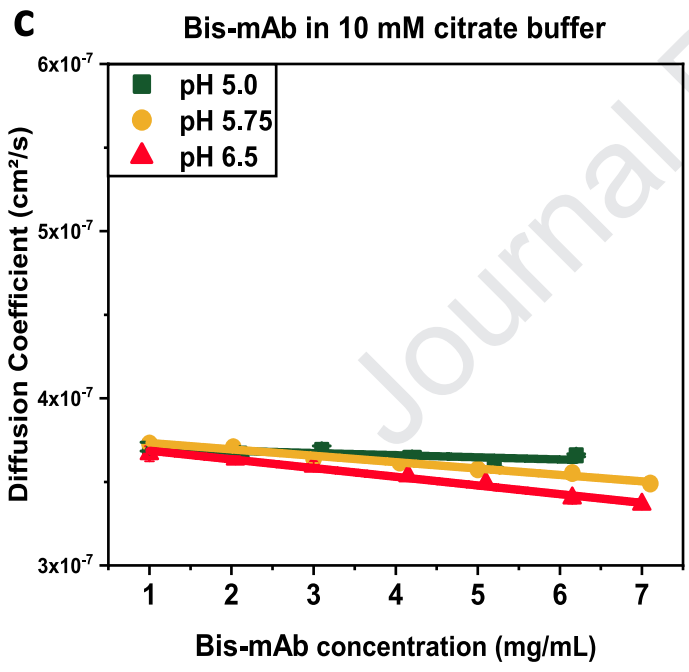

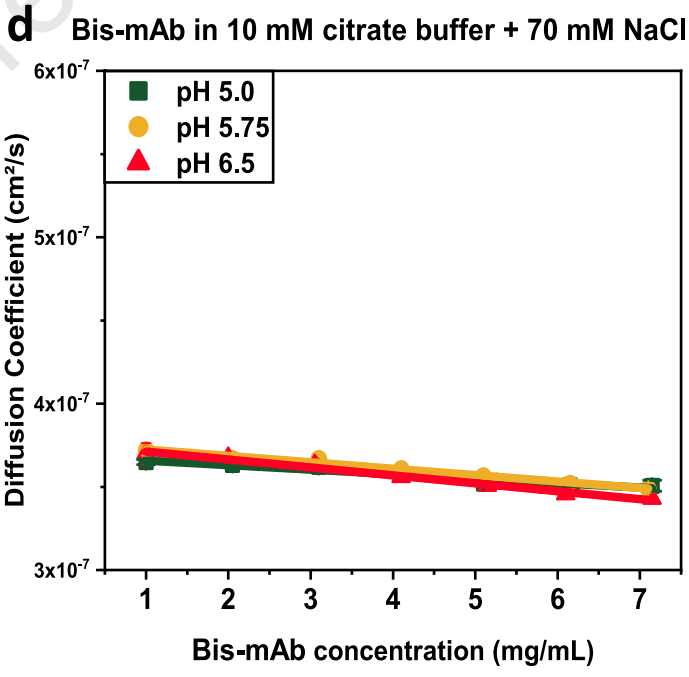

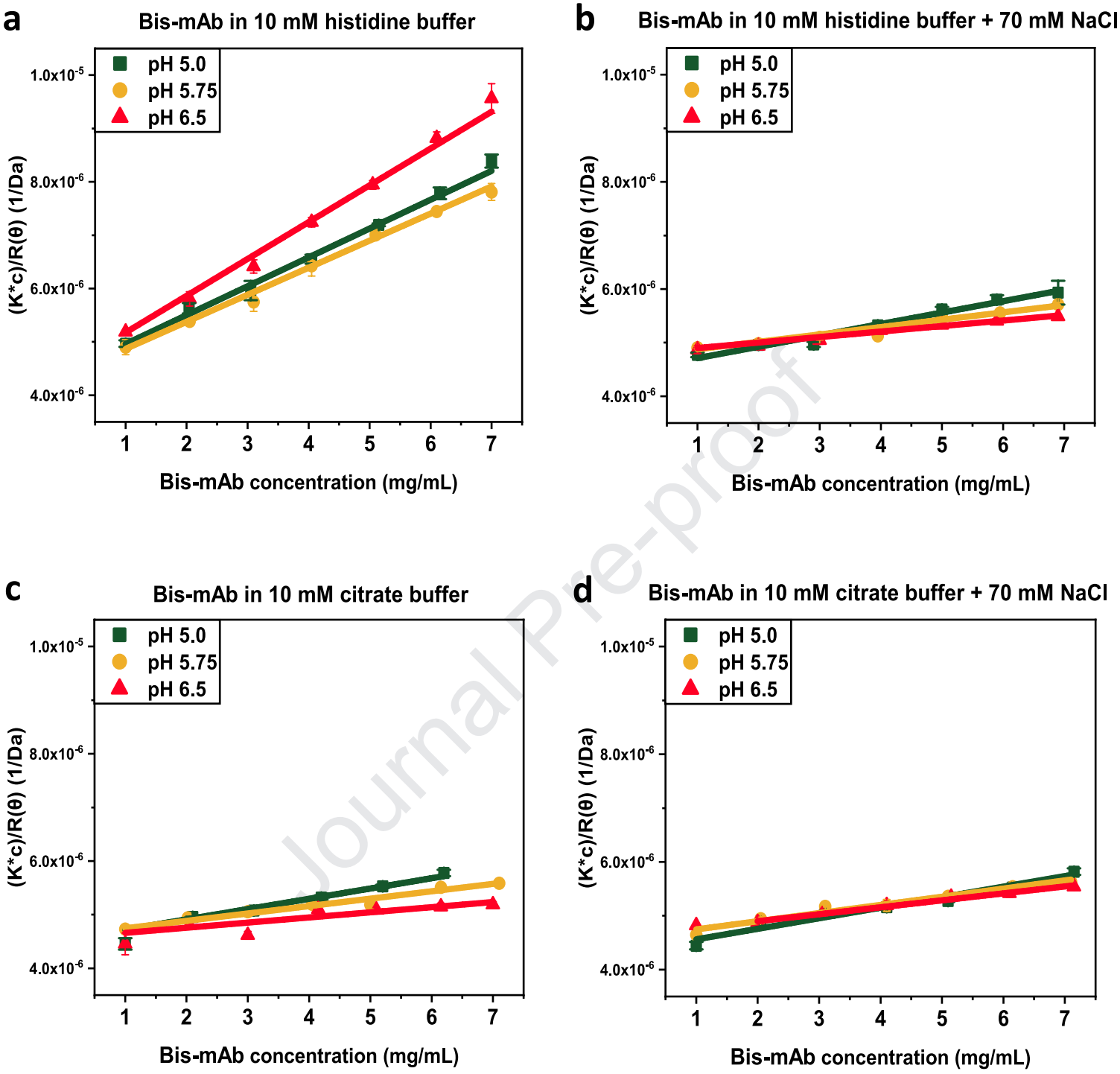

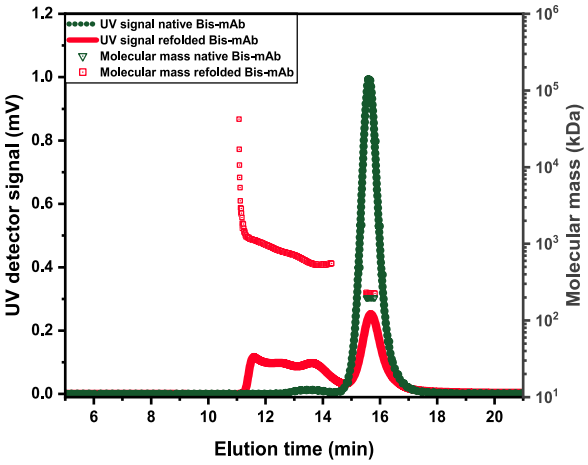

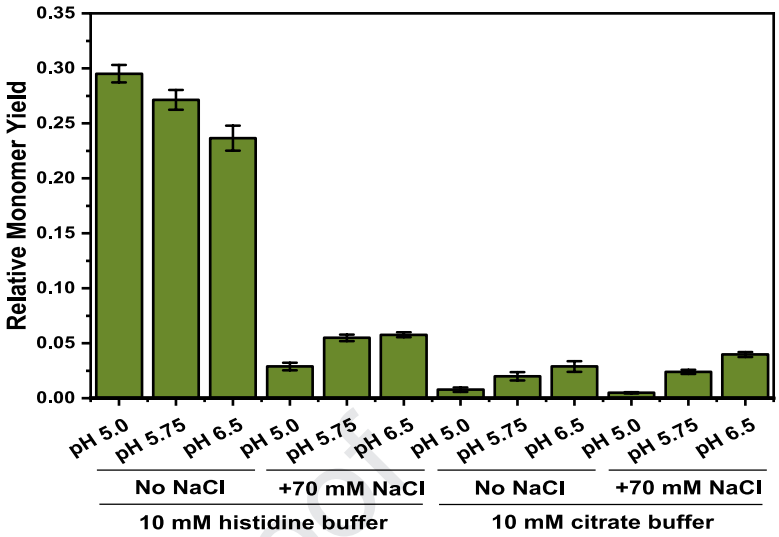

a

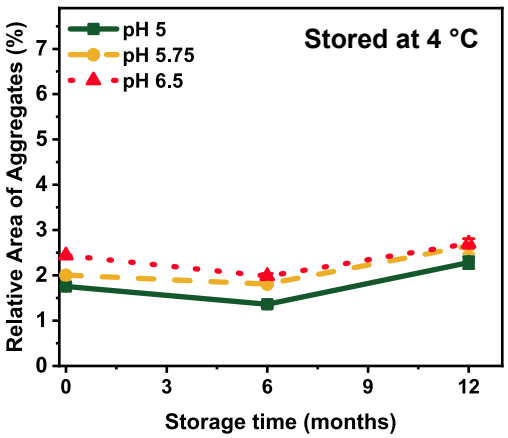

b

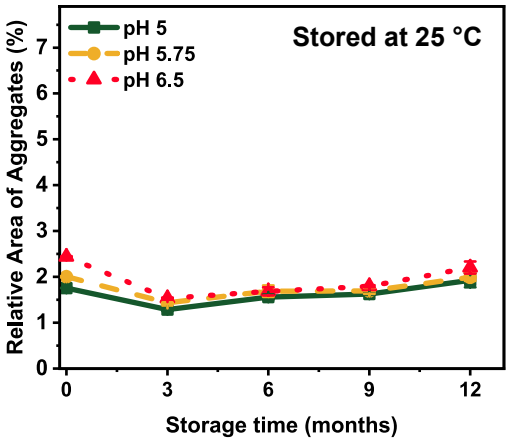

c

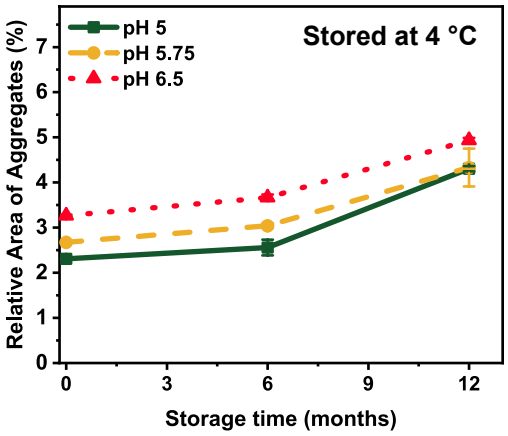

d

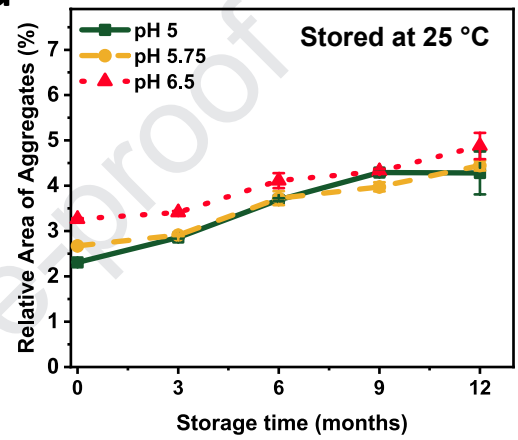

e

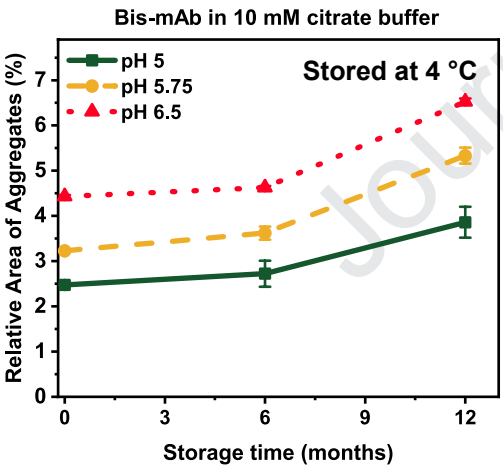

f

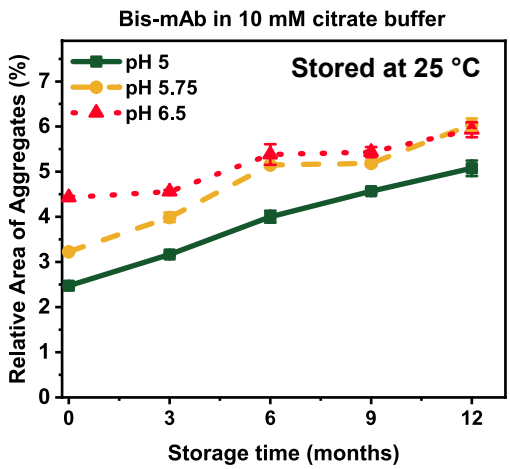

g

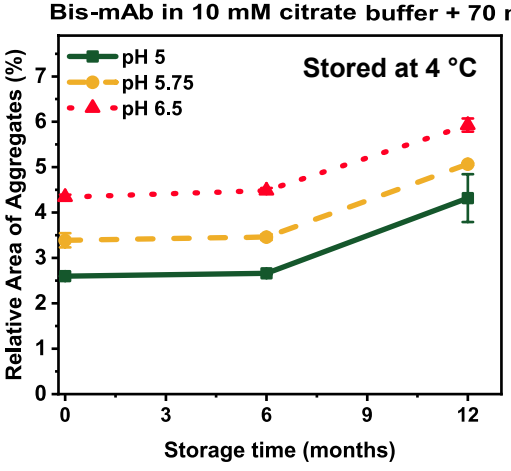

h

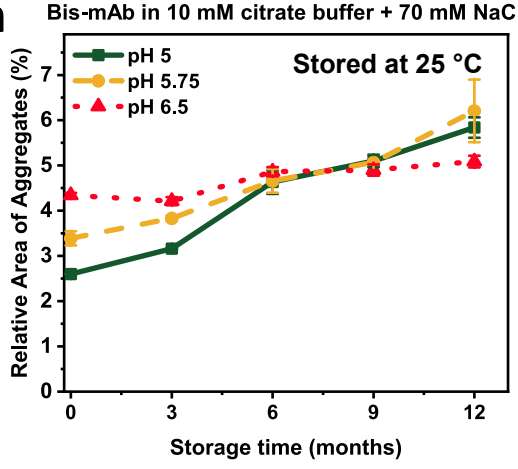

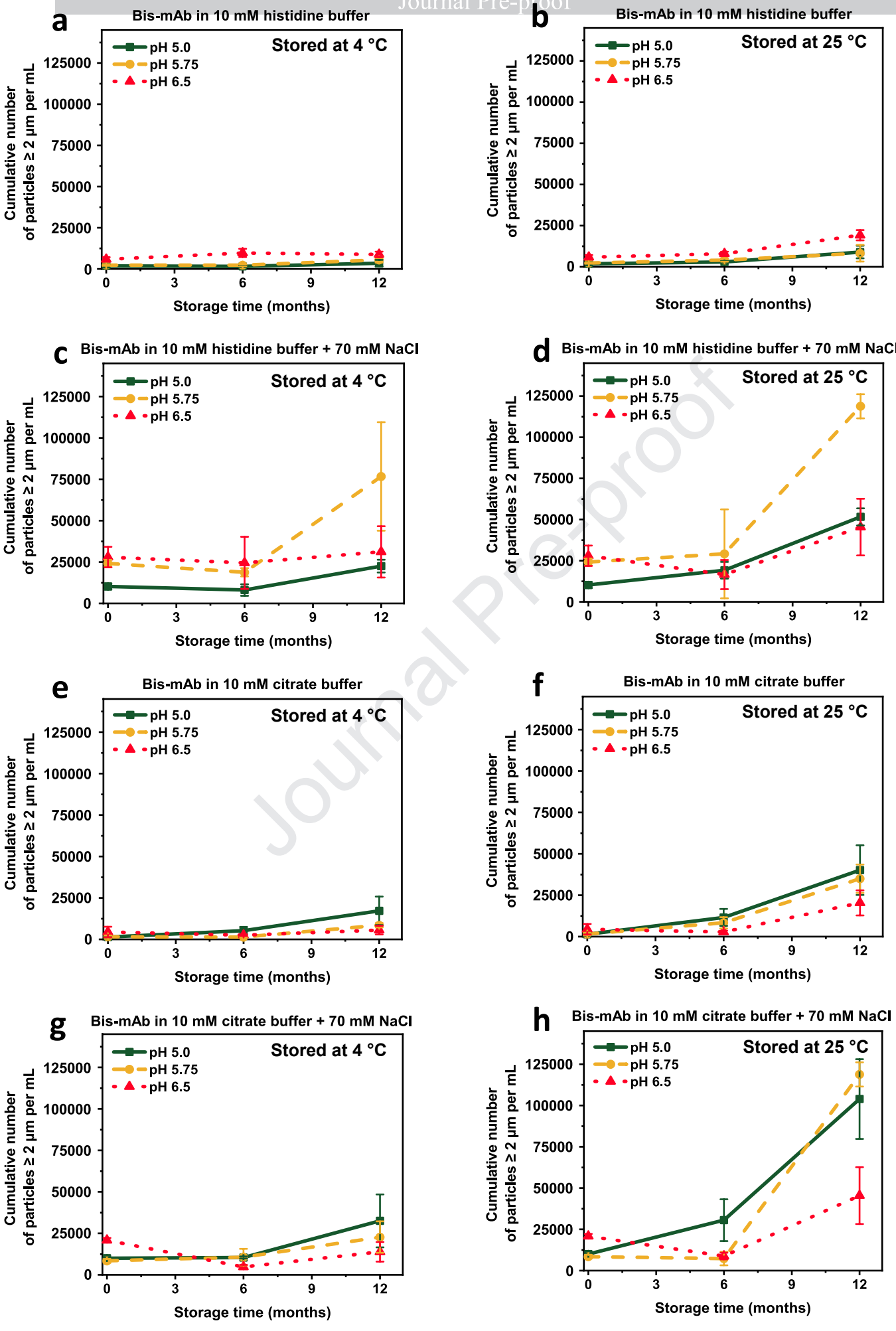

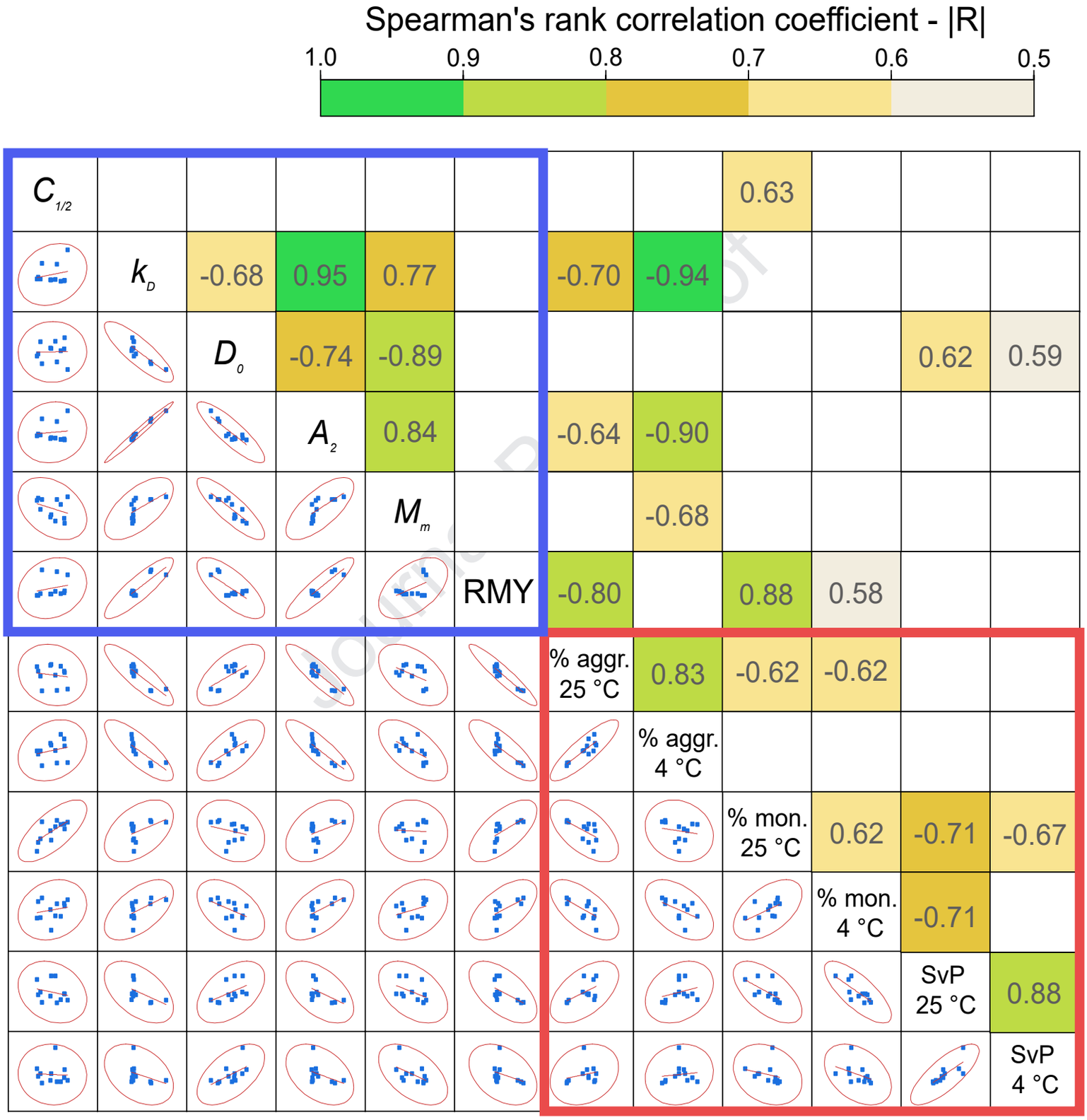
Spearman's rank correlation coefficient - |R|
1.0
0.9
0.8
0.7
0.6
0.5
$C_{1/2}$
k_D
D_0
A_2
M_m
RMY
% aggr. 25 °C
% aggr. 4 °C
% mon. 25 °C
% mon. 4 °C
SvP 25 °C
SvP 4 °C
-0.68
0.95
0.77
-0.70
-0.94
0.63
-0.74
-0.89
0.62
0.59
-0.64
-0.90
0.84
-0.68
-0.80
0.88
0.58
0.83
-0.62
-0.62
0.62
-0.71
-0.67
-0.71
0.88